# NATIONAL ADVISORY COMMITTEE FOR AERONAUTICS

TECHNICAL NOTE 2156

THEORETICAL CALCULATIONS OF THE LATERAL FORCE AND YAWING

MOMENT DUE TO ROLLING AT SUPERSONIC SPEEDS FOR SWEPTBACK

TAPERED WINGS WITH STREAMWISE TIPS

SUPERSONIC LEADING EDGES

By Sidney M. Harmon and John C. Martin

Langley Aeronautical Laboratory
Langley Air Force Base, Va.

NACA

Washington
July 1950

NATIONAL ADVISORY COMMITTEE FOR AERONAUTICS

TECHNICAL NOTE 2156

THEORETICAL CALCULATIONS OF THE LATERAL FORCE AND YAWING

MOMENT DUE TO ROLLING AT SUPERSONIC SPEEDS FOR SWEPTBACK

TAPERED WINGS WITH STREAMWISE TIPS ·

SUPERSONIC LEADING EDGES

By Sidney M. Harmon and John C. Martin

SUMMARY

Theoretical results are obtained, by means of the linearized theory, for the lateral force and yawing moment due to combined angle of attack and roll. The thin wings considered are tapered and have leading and trailing edges which are each swept at a constant angle; the tips are parallel to the center section. Further restrictions are that the leading edges are supersonic (the velocity component normal to the leading edge is supersonic) and the Mach lines from either tip do not intersect the remote tip. The trailing edges may be either supersonic or subsonic provided that the taper ratio is equal to or less than one.

Design curves are presented which permit rapid estimation of the two stability derivatives, rate of change of lateral force and yawing moment with roll C_{Y_p} and C_{n_p}, respectively, for given values of aspect ratio, taper ratio, Mach number, and leading-edge sweep. These design curves are given relative to the body axes with the origin located at the projection of the leading edge of the tip section on the center section. The conversion to stability axes with moments about an arbitrary axis can be accomplished by use of a simple formula given herein.

INTRODUCTION

One of the important derivatives required in the prediction of the lateral stability of airplanes is the rate of change of yawing moment with roll. Theoretical results for this derivative C_{n_p} and also for the derivative expressing the rate of change of lateral force with roll C_{Y_p} at supersonic speeds have been reported in a number of papers for thin wings having particular plan forms. These papers include

references 1 and 2 for triangular plan forms, reference 3 for rectangular wings, reference 4 for wings of zero taper ratio having sweptback, subsonic leading edges, and reference 5 for sweptback tapered wings with streamwise tips and subsonic leading edges (the component of velocity normal to the leading edge is subsonic).

In the present paper, the linearized theory is used to obtain the derivatives C_{n_p} and C_{Y_p} for thin wings at supersonic speeds. The wings considered have conventional taper ratios, the leading and trailing edges are each swept at a constant angle, and the tips are parallel to the center section. The results are valid only for a range of supersonic speeds for which the leading edge is supersonic (the component of velocity normal to the edge is supersonic). The trailing edges may be either supersonic or subsonic provided that subsonic edges do not affect the tip edges. A further restriction is that the Mach lines from either tip do not intersect the remote tip.

SYMBOLS

x,y	rectangular coordinates (figs. 1 and 2(a))
v_n	induced flow velocity along Y-axis
V	undisturbed flight velocity
p	angular velocity about the X-axis
ρ	density of air
a	speed of sound
M	stream Mach number (V/a)
$B = \sqrt{M^2 - 1}$	
μ	Mach angle $\left(\sin^{-1} \frac{1}{M}\right)$
α	wing angle of attack in steady flight, radians
Λ	sweepback angle of wing leading edge
$m = \cot \Lambda$	
$m' = B \cot \Lambda$	

ϕ disturbance-velocity potential on upper surface of airfoil

λ ratio of tip chord to root chord (taper ratio)

b   wing span

S   total wing area

s_n distance to tip edge

A   aspect ratio

$A' = BA$

x_{cg} distance from wing apex to center of gravity in root chords measured positively as indicated in figure 2(b)

F   induced suction force on wing tip per unit length of tip

G   function of x given by equation (1)

$$C_l = \frac{\text{Rolling moment}}{\frac{\rho}{2} V^2 S b}$$

$$C_Y = \frac{\text{Lateral force}}{\frac{\rho}{2} V^2 S}$$

$$C_n = \frac{\text{Yawing moment}}{\frac{\rho}{2} V^2 S b}$$

$$C_{n_p} = \left(\frac{\partial C_n}{\partial \frac{pb}{2V}} \right)_{\frac{pb}{2V} \to 0}$$ with respect to body axes with origin located x_{cg} root chords from leading edge of center section

$$\left(C_{n_p} \right)_1 = \left(\frac{\partial C_n}{\partial \frac{pb}{2V}} \right)_{\frac{pb}{2V} \to 0}$$ with respect to body axes with origin located at projection of leading edge of tip section on center section (fig. 2(a))

$$C_{n_p}{}' = \left(\frac{\partial C_n}{\partial \frac{pb}{2V}}\right)_{\frac{pb}{2V} \to 0}$$

with respect to stability axes with origin located x_{cg} root chords from leading edge of center section

$$C_{l_p} = \left(\frac{\partial C_l}{\partial \frac{pb}{2V}}\right)_{\frac{pb}{2V} \to 0}$$

$$C_{Y_p} = \left(\frac{\partial C_Y}{\partial \frac{pb}{2V}}\right)_{\frac{pb}{2V} \to 0}$$

with respect to body axes

Subscripts:

TE   refers to wing trailing edge

a,p   contributions caused by angle of attack and rolling motions, respectively

ANALYSIS

Scope

The wing configurations considered in the analysis are shown in figure 1. These wings have streamwise tips and sweptback leading edges, although the trailing edges may be either sweptback or sweptforward. The results are valid only for a range of supersonic speeds for which the leading edge is supersonic. The trailing edge may be either subsonic or supersonic provided that the taper ratio is equal to or less than one. For subsonic trailing edges the Kutta condition is assumed to be satisfied along the trailing edges. A further restriction on these wings is that the Mach lines from either tip do not intersect the remote tip. The analysis is based upon linearized theory; therefore, the results are subject to the restrictions of this theory.

The derivation of the stability derivatives is made initially with reference to the body axes which are fixed in the wing with the origin located at the projection of the leading edge of the tip on the center section (fig. 2(a)). The transformation of the stability derivatives to a system of stability axes (fig. 2(b)) is discussed in the section entitled "Derivation of Formulas."

Basic Considerations

The stability derivatives are determined from integrations of the forces and moments over the wing. If skin friction is neglected, these forces and moments arise from pressures on the wing surfaces and from suction forces along the edges of the wing. A lifting wing with streamwise tips or subsonic leading edges will induce suction forces along the subsonic leading edges and along the streamwise tips. These forces arise because of the flow from the bottom to the top surfaces. This analysis is concerned only with the derivatives C_{Y_p} and C_{n_p}. For these derivatives with respect to the body axes, the lateral forces and yawing moments are produced only by suction forces along the edges of the wing. Since in this analysis the leading edges are supersonic, no suction forces are induced along these edges; thus, the determination of the derivatives C_{Y_p} and C_{n_p} in the cases considered has involved only the evaluation of unbalanced suction forces along the wing tips. The Kutta condition is assumed to be satisfied along the subsonic trailing edges.

The suction forces along an edge of infinitesimally small thickness can be evaluated theoretically by a method suggested in reference 6 for incompressible flow and modified for compressibility effects in reference 7. If this method is used, the suction force varies as the square of the induced flow velocity around the edge. In general, in the linearized theory the induced velocity varies directly as the magnitude of a given motion. Thus for constant angle of attack, the induced velocity around the edge is proportional to α; and in a rolling motion, the induced velocity is proportional to p. For constant angle of attack and constant rate of roll, the suction forces vary as the squares of α and p, respectively. These forces are in the opposite direction and of the same magnitude; thus no lateral force or yawing moment is developed. For combined angle of attack and roll, unbalanced suction forces occur that vary as the cross product of α and p; consequently, these forces or the associated stability derivatives cannot be obtained by superposing separately the components due to each motion. The present analysis takes into account this general condition of simultaneous rolling and vertical motions.

Derivation of Formulas

According to the methods of references 6 and 7, the induced surface velocity normal to the wing tip is expressed as

$$(v_n)_{s_n \to 0} = \frac{G}{\sqrt{s_n}} \tag{1}$$

where G is a function of x only and s_n is the distance to the tip
edge. Then the suction force per unit length of tip is

$$F = \pi \rho G^2 \qquad (2)$$

for streamwise tips.

The induced surface velocity normal to the tips of a wing simul-
taneously in roll and at a given angle of attack α is given by

$$(v_n)_{\alpha+p} = \left(\frac{\partial \phi}{\partial y}\right)_\alpha + \left(\frac{\partial \phi}{\partial y}\right)_p \qquad (3)$$

where the quantities are evaluated in the immediate vicinity of the wing
tip, that is for $s_n \to 0$. The potential functions ϕ_α and ϕ_p for use
in equation (3) were obtained from table I (regions 3 and 5) of refer-
ence 8. By utilizing these expressions for the potential functions and
by substituting for v_n in equation (1), the function G is determined.
The suction force per unit length along the wing tip F is then obtained
from equation (2).

If the origin of the body axes is taken at the projection of the
leading edge of the tip on the center section (fig. 2(a)), the non-
dimensional forms of the expressions for the derivatives are as follows:

$$C_{Y_p} = \frac{4 \int_{Tip} F\, dx}{\rho V S b p} \qquad (4)$$

$$\left(C_{n_p}\right)_1 = -\frac{4 \int_{Tip} F x\, dx}{\rho V S b^2 p} \qquad (5)$$

where the integrals are evaluated along both wing tips.

Formulas for the derivatives C_{Y_p} and $\left(C_{n_p}\right)_1$ are given in the
appendix. These formulas are for the two different plan-form configura-
tions which occur, that is, for the cases where the foremost Mach line

from the center section cuts the wing trailing edge or the tip. (See fig. 3.)

The derivative $\left(C_{n_p}\right)_1$ is readily transformed to a system of body axes with its origin at an arbitrary point along the center section. Thus, if the origin of the axes is located x_{cg} root chords from the leading edge of the center section, the following equation results

$$C_{n_p} = \left(C_{n_p}\right)_1 + \left[\frac{2x_{cg}}{A(1 + \lambda)} - \frac{1}{2m}\right]C_{Y_p} \tag{6}$$

The nondimensional stability derivatives C_{Y_p} and $\left(C_{n_p}\right)_1$, which were derived with reference to body axes with the origin located at the projection of the leading edge of·the tip on the center section (fig. 2(a)), may be transformed to apply to stability axes with the origin at an arbitrary point along the center section. (See fig. 2(b).)

The transformation formulas for conversion from body axes to stability axes are given in reference 9 and also in table II of reference 3 where terms of the order of α^2 are omitted. A consideration of these formulas and the derivatives involved therein shows that, to the first order in α, the conversion formulas from body axes to stability axes are

$$C_{Y_p}' = C_{Y_p} \tag{7}$$

$$C_{n_p}' = C_{n_p} - \alpha C_{l_p} = \left(C_{n_p}\right)_1 + \left[\frac{2x_{cg}}{A(1 + \lambda)} - \frac{1}{2m}\right]C_{Y_p} - \alpha C_{l_p} \tag{8}$$

where the primes refer to the stability axes with the origin located along the center section at an arbitrary distance x_{cg} root chords from the leading edge.

The derivative C_{l_p} which appears in equation (8), if obtained to the first order in α, has the same value either with respect to body axes or with respect to stability axes. Values for C_{l_p} for use in equation (8) may be obtained from reference 8 for all the wing configurations considered in this paper, except for a special case. This special case occurs if the Mach line from the leading edge of a tip section intersects the remote half-wing coincidentally as the Mach line from the leading edge of the center section intersects the tip section. (See fig. 1(b).)

RESULTS AND DISCUSSION

The results of the calculations are presented in figures 4 and 5 in the form C_{Y_p}/α and $\left(C_{n_p}\right)_1/B\alpha$ plotted against $B \cot \Lambda$ for various values of BA and λ. The derivatives C_{Y_p} and $\left(C_{n_p}\right)_1$ were computed from equations (A1) and (A5) and from equations (A2) and (A6), respectively.

If in figures 4 and 5 the Mach number and B are constant, the data in these figures indicate directly the variations, respectively, of the derivatives C_{Y_p} and $\left(C_{n_p}\right)_1$ with the angle of sweep of the leading edge, aspect ratio, and taper ratio. With B held constant, the data in figures 4 and 5 indicate that as the leading-edge sweep angle is increased (decreasing values of $\beta \cot \Lambda$) C_{Y_p} increases positively and $\left(C_{n_p}\right)_1$ increases negatively. The data in figures 4 and 5 also indicate that, with B, λ, and Λ constant, C_{Y_p} and $\left(C_{n_p}\right)_1$ increase in magnitude with decreasing aspect ratio and, with B, A, and Λ constant, C_{Y_p} and $\left(C_{n_p}\right)_1$ increase in magnitude with increasing taper ratio.

Figure 6 presents some illustrative results for the derivative C_{n_p}' with respect to the stability axes. These data illustrate the variations in C_{n_p}' with Mach number, aspect ratio, sweepback, and taper ratio. For these illustrative results the origin of the stability axes is assumed to be at the leading edge of the center section $\left(x_{cg} = 0\right)$. Since the origin is at the leading edge of the center section, the sweep effect shown is considerably greater than would probably be encountered in an actual airplane design where the longitudinal location of the center of gravity would probably be near the wing center of pressure. The effect on C_{n_p}' of shifting the origin of the stability axes is not shown in figure 6 but is readily obtained from an examination of equation (8). From equation (8) shifting the origin of the stability axes rearward $\left(\text{increasing } x_{cg}\right)$ is noted to result in a change in the yawing-moment coefficient equal to

$$\frac{2x_{cg}\left(C_{Y_p}\right)}{A(1 + \lambda)}$$

Thus, for the usual case in which C_{Y_p} is positive, an increase in x_{cg} contributes a positive increment to C_{n_p}. The data for C_{n_p}' given in figure 6 were computed from equation (8), in which the values for C_{Y_p}

and $\left(C_{n_p}\right)_1$ were obtained from figures 4 and 5, respectively, and the values for C_{l_p} were obtained from figure 10 of reference 8.

The results of the present investigation have been derived on the assumptions of zero thickness and small disturbances. Theoretically, infinite lateral perturbation velocities are induced along the tips. These velocities cause infinite perturbation pressures which, when acting on an edge of zero thickness, yield a finite suction force. In the actual flow, however, the infinite pressures are never realized; but the drop in pressure tends to be compensated by the increased force which results from the finite thickness of the actual side edge (wing tip). These points are discussed in slightly more detail in reference 2.

CONCLUDING REMARKS

General expressions have been obtained by means of the linearized theory for the lateral force and yawing moment due to rolling for sweptback tapered wings with streamwise tips and supersonic leading edges. The trailing edges are swept and may be either supersonic or subsonic provided that the taper ratio is equal to or less than one. A further restriction on these wings is that the Mach lines from either tip do not intersect the remote tip. The analysis is based upon linearized theory; therefore, the results are subject to the restrictions of this theory.

The results of the investigation were presented in the form of generalized design curves for rapid estimation of the two stability derivatives, the rate of change of lateral force and of yawing moment with roll C_{Y_p} and C_{n_p}, respectively. Some specific variations of the more important derivative C_{n_p} with Mach number, aspect ratio, leading-edge sweep angle, and taper ratio were also presented.

Langley Aeronautical Laboratory
    National Advisory Committee for Aeronautics
        Langley Air Force Base, Va., May 18, 1950

APPENDIX

FORMULAS FOR C_{Y_p} AND $\left(C_{n_p}\right)_1$

Formulas are given for C_{Y_p} and $\left(C_{n_p}\right)_1$ with respect to the body axes with its origin located at the projection of the leading edge of the tip section on the center section for thin tapered wings with swept leading and trailing edges and with streamwise tips. The leading edges are supersonic and the Mach lines from either tip do not intersect the remote tip. These formulas for the two cases illustrated in figure 3 are limited by the following conditions:

$$B \cot \Lambda \gtreqless 1$$

$$B \cot \Lambda_{TE} \gtreqless 1 \quad \text{or} \quad B \cot \Lambda_{TE} < 0$$

and

$$BA > \frac{2\lambda}{1 + \lambda}$$

Case I - Foremost Mach line from center section cuts wing trailing edge.- For case I for which the foremost Mach line from the center section cuts the wing trailing edge, the equations for C_{Y_p} and $\left(C_{n_p}\right)_1$ are

$$C_{Y_p} = \frac{64\alpha\lambda^2 m' \left[9A'(1 + \lambda)(m' - 1) - 8\lambda m'\right]}{9\pi(A')^2(m' - 1)^2(1 + \lambda)^3} \qquad (A1)$$

$$\left(C_{n_p}\right)_1 = \frac{-256\alpha B\lambda^3 m' \left[A'(1 + \lambda)(m' - 1) - \lambda m'\right]}{3\pi(A')^3(m' - 1)^2(1 + \lambda)^4} \qquad (A2)$$

When the leading edge is straight $(m = \infty)$, equations (A1) and (A2) reduce to the following expressions:

$$C_{Y_p} = \frac{64\alpha\lambda^2 \left[9A'(1 + \lambda) - 8\lambda\right]}{9\pi(A')^2(1 + \lambda)^3} \qquad (A3)$$

$$\left(C_{n_p}\right)_1 = -\frac{256\alpha B\lambda^3\left[A'(1+\lambda) - \lambda\right]}{3\pi(A')^3(1+\lambda)^4} \tag{A4}$$

Case II — Foremost Mach line from center section cuts wing tip.- For case II for which the foremost Mach line from the center section cuts the wing tip, the equations for C_{Y_p} and $\left(C_{n_p}\right)_1$ are

$$C_{Y_p} = \frac{4\alpha}{9\pi(A')^2 m'(m'+1)^2}\left\{-(A')^3(m'-1)(14m'+6) + \right.$$

$$\left.16m'\lambda\left[\frac{3A'(3m'+1)}{1+\lambda} + \frac{3A'm'\lambda(3m'-1)}{(1+\lambda)^2} - \frac{8m'\lambda^2}{(1+\lambda)^3}\right]\right\} \tag{A5}$$

$$\left(C_{n_p}\right)_1 = \frac{4\alpha B}{9\pi(A')^3(m')^3(m'+1)^2}\left\{(A')^4(m'-1)^2(2m'+1) + \right.$$

$$\left.16(m')^2\lambda^2\left[-\frac{3(A')^2(3m'+1)}{(1+\lambda)^2} - \frac{4A'm'\lambda(3m'-1)}{(1+\lambda)^3} + \frac{12(m')^2\lambda^2}{(1+\lambda)^4}\right]\right\} \tag{A6}$$

When the leading edge is straight $(m = \infty)$, the expressions for C_{Y_p} and $\left(C_{n_p}\right)_1$, given by equations (A5) and (A6), reduce to the same corresponding formulas as those obtained previously for case I. Thus, C_{Y_p} and $\left(C_{n_p}\right)_1$ for case II when the leading edge is straight are given by equations (A3) and (A4), respectively.

REFERENCES

1. Ribner, Herbert S.: The Stability Derivatives of Low-Aspect-Ratio
   Triangular Wings at Subsonic and Supersonic Speeds. NACA TN 1423,
   1947.

2. Ribner, Herbert S., and Malvestuto, Frank S., Jr.: Stability Deriva-
   tives of Triangular Wings at Supersonic Speeds. NACA Rep. 908, 1948.

3. Harmon, Sidney M.: Stability Derivatives at Supersonic Speeds of Thin
   Rectangular Wings with Diagonals ahead of Tip Mach Lines. NACA
   Rep. 925, 1949.

4. Malvestuto, Frank S., Jr., and Margolis, Kenneth: Theoretical
   Stability Derivatives of Thin Sweptback Wings Tapered to a Point
   with Sweptback or Sweptforward Trailing Edges for a Limited Range
   of Supersonic Speeds. NACA TN 1761, 1949.

5. Margolis, Kenneth: Theoretical Calculations of the Lateral Force and
   Yawing Moment Due to Rolling at Supersonic Speeds for Sweptback
   Tapered Wings with Streamwise Tips. Subsonic Leading Edges. NACA
   TN 2122, 1950.

6. Von Kármán, Th., and Burgers, J. M.: General Aerodynamic Theory –
   Perfect Fluids. Theory of Airplane Wings of Infinite Span. Vol. II
   of Aerodynamic Theory, div. E, ch. II, sec. 10; W. F. Durand, ed.,
   Julius Springer (Berlin), 1935, pp. 48–53.

7. Brown, Clinton E.: Theoretical Lift and Drag of Thin Triangular
   Wings at Supersonic Speeds. NACA Rep. 839, 1946.

8. Harmon, Sidney M., and Jeffreys, Isabella: Theoretical Lift and
   Damping in Roll of Thin Wings with Arbitrary Sweep and Taper at
   Supersonic Speeds. Supersonic Leading and Trailing Edges. NACA
   TN 2114, 1950.

9. Glauert, H.: A Non-Dimensional Form of the Stability Equations of
   an Aeroplane. R. & M. No. 1093, British A.R.C., 1927.
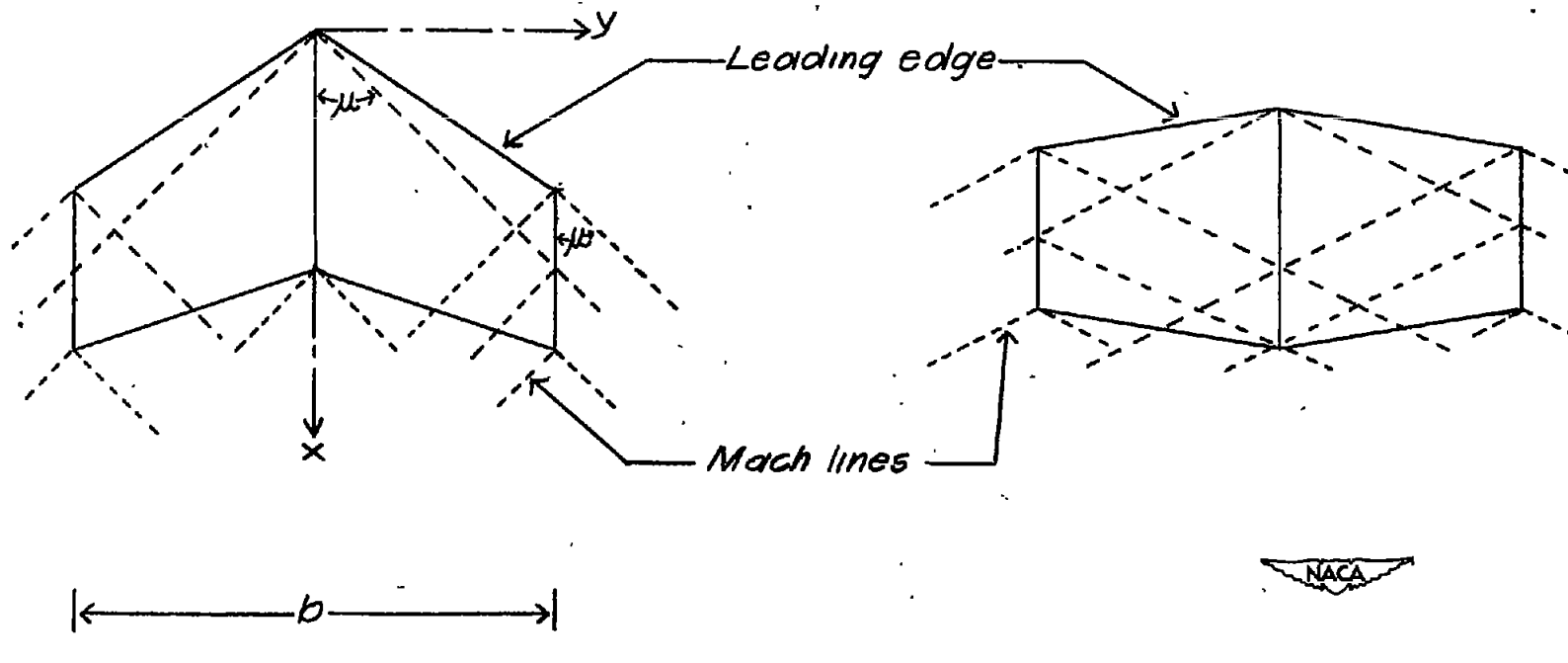
(a) Sweptback leading and trailing edges.

(b) Sweptback leading edge and sweptforward trailing edge.

Figure 1.- Wing configurations considered in analysis. Supersonic leading edges; streamwise tips. Note that Mach lines from leading edge of center section may intersect either the tip or trailing edge and that Mach line from either tip does not intersect the remote tip.

$$B \cot \Lambda \gtreqless 1, \quad B \cot \Lambda_{TE} \gtreqless 1 \quad \text{or} \quad B \cot \Lambda_{TE} < 0, \quad \text{and} \quad BA > \frac{2\lambda}{1 + \lambda}.$$
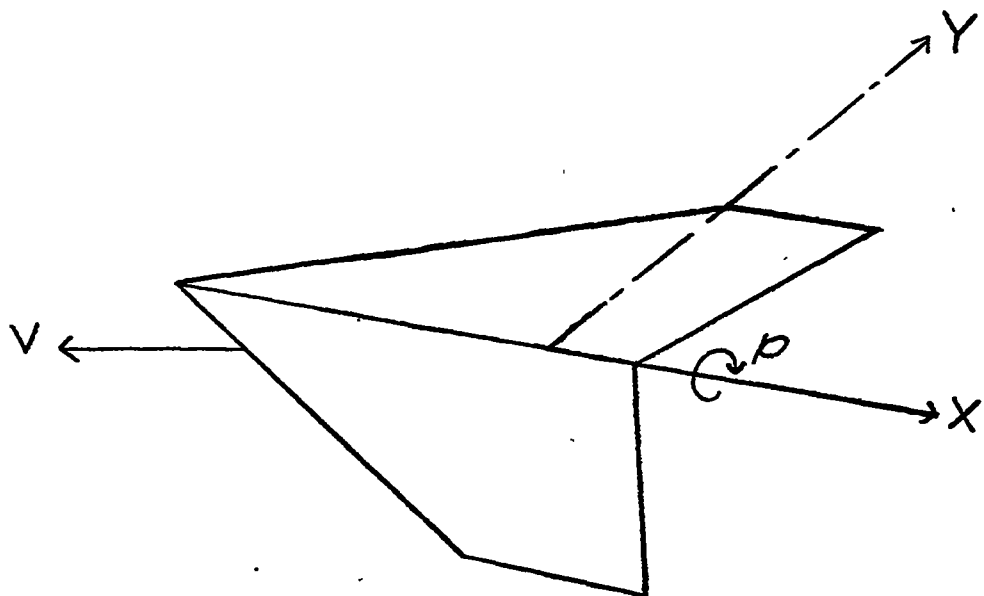
(a) Notation and body axes used in analysis. Origin is located at projection of leading edge of tip on center section.
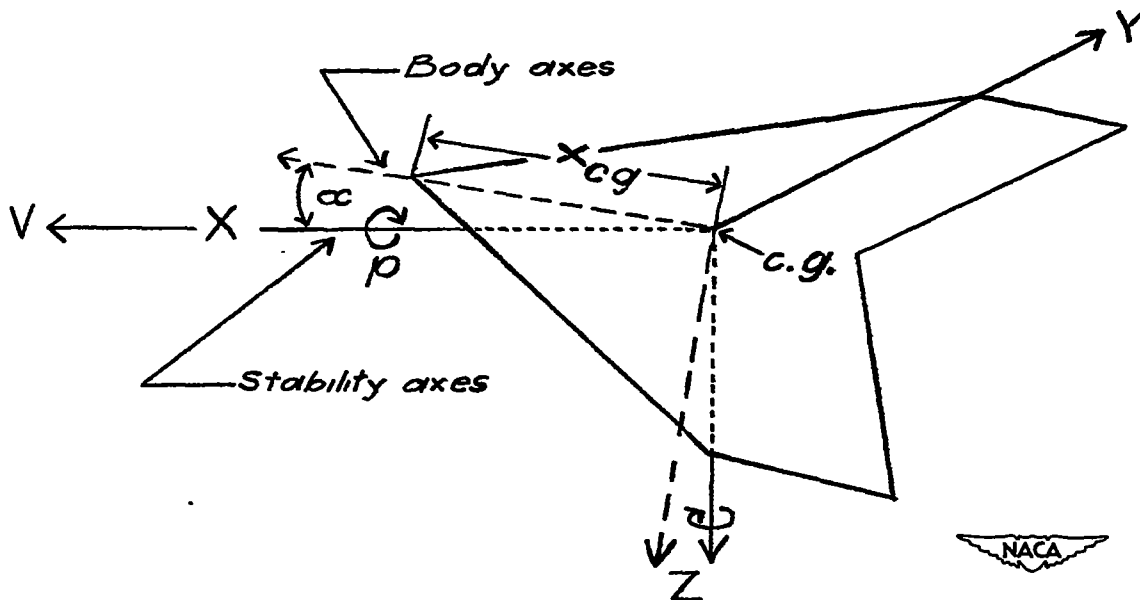
(b) Stability axes. (Corresponding body axes dashed for comparison.)

Figure 2.- Systems of axes.
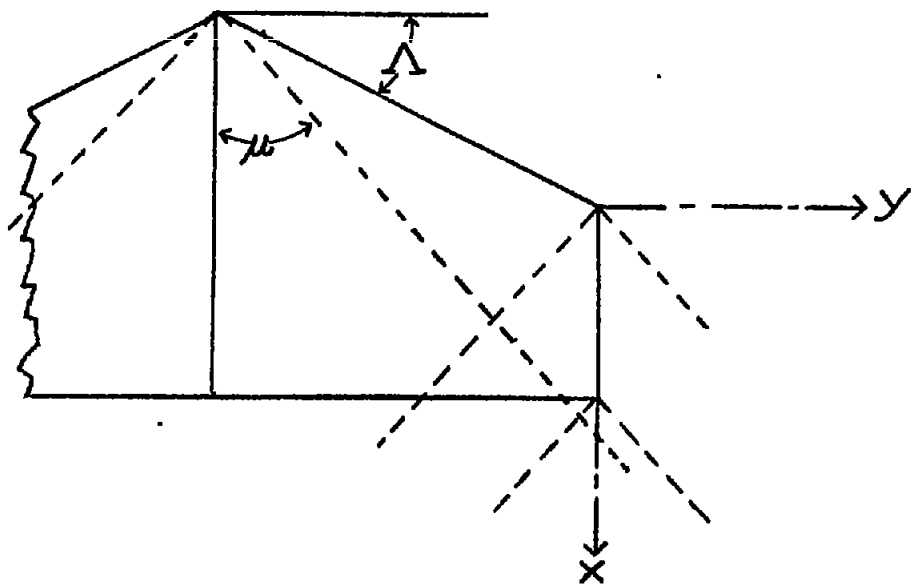
(a) Case I.
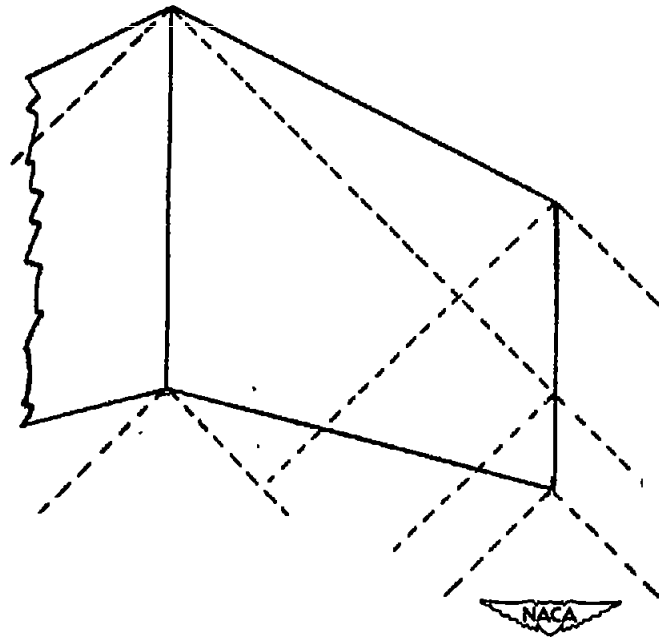
(b) Case II.

Figure 3.- Two types of plan-form configuration used for derivation of
formulas for lateral-force and yawing-moment derivatives.
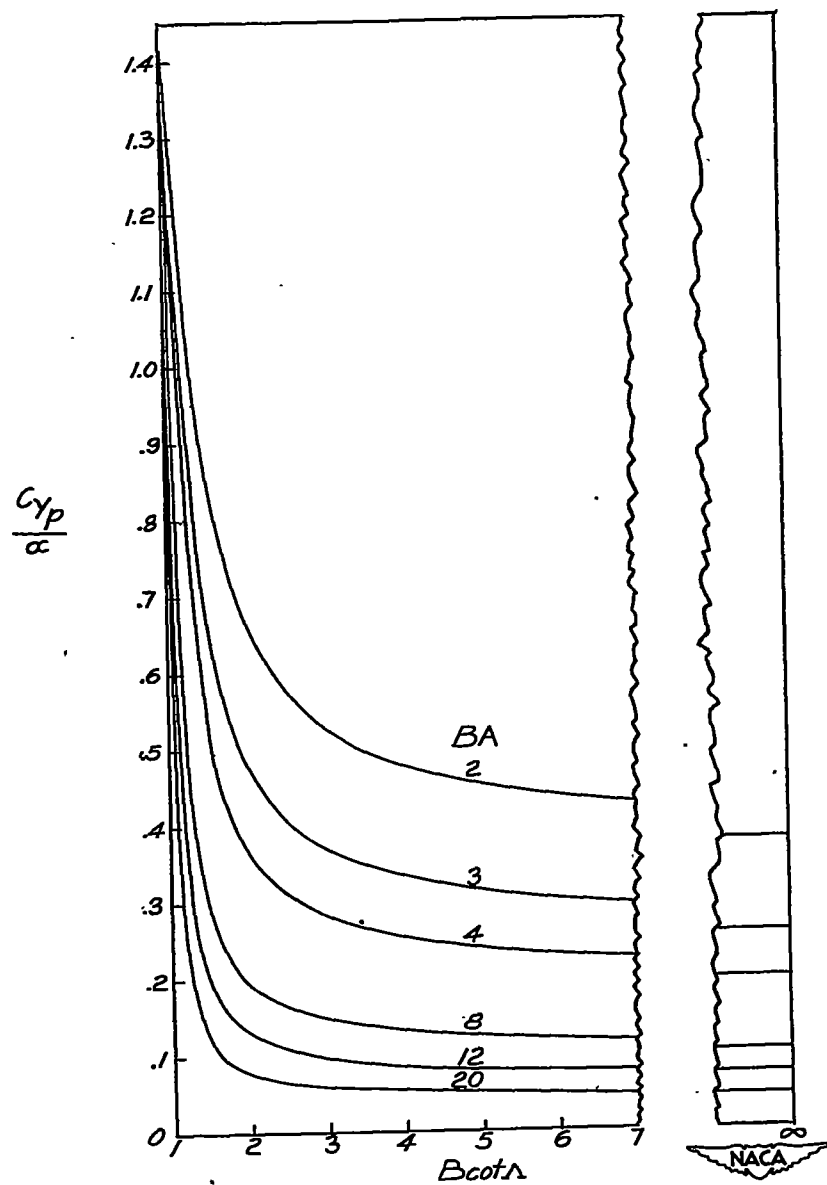
(a) Taper ratio $\lambda = 0.25$.

Figure 4.- Variation of C_{y_p}/α with sweepback-angle parameter for various aspect-ratio parameters and taper ratios.
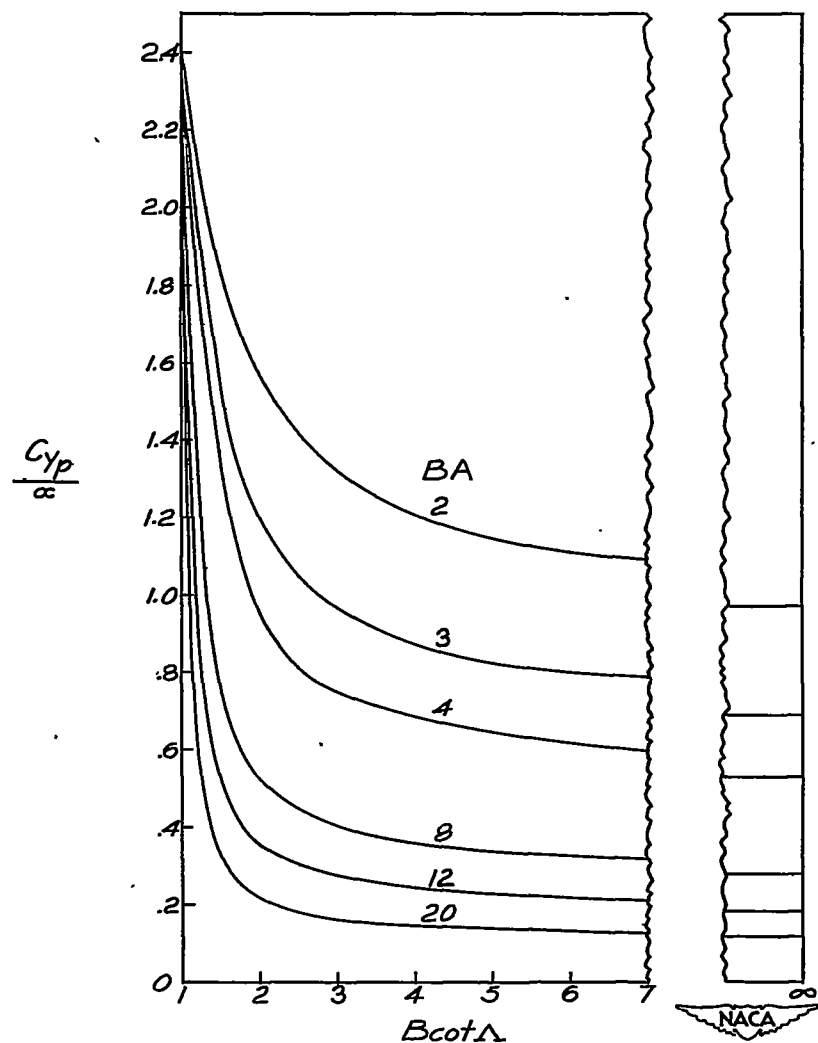
(b) Taper ratio $\lambda = 0.50.$

Figure 4.- Continued.
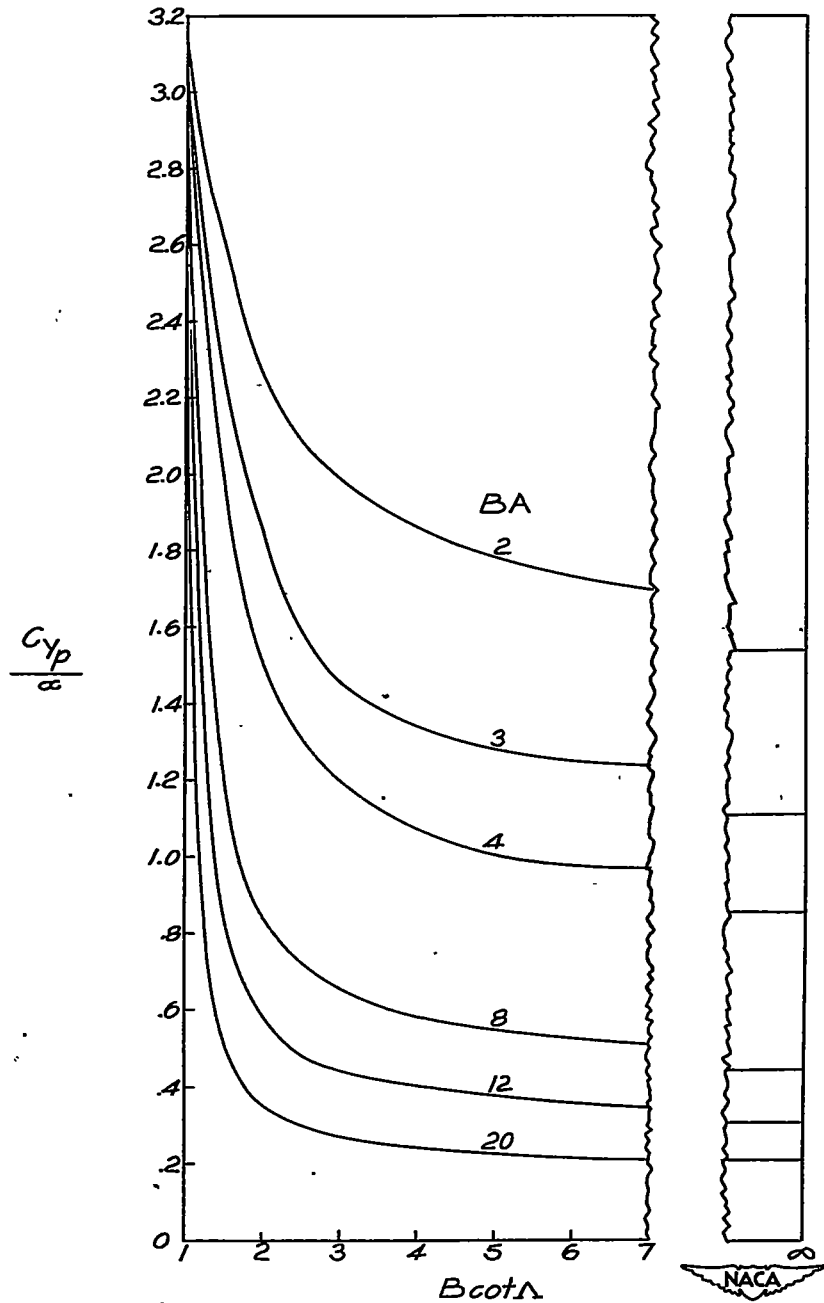
(c) Taper ratio λ = 0.75.

Figure 4.- Continued.
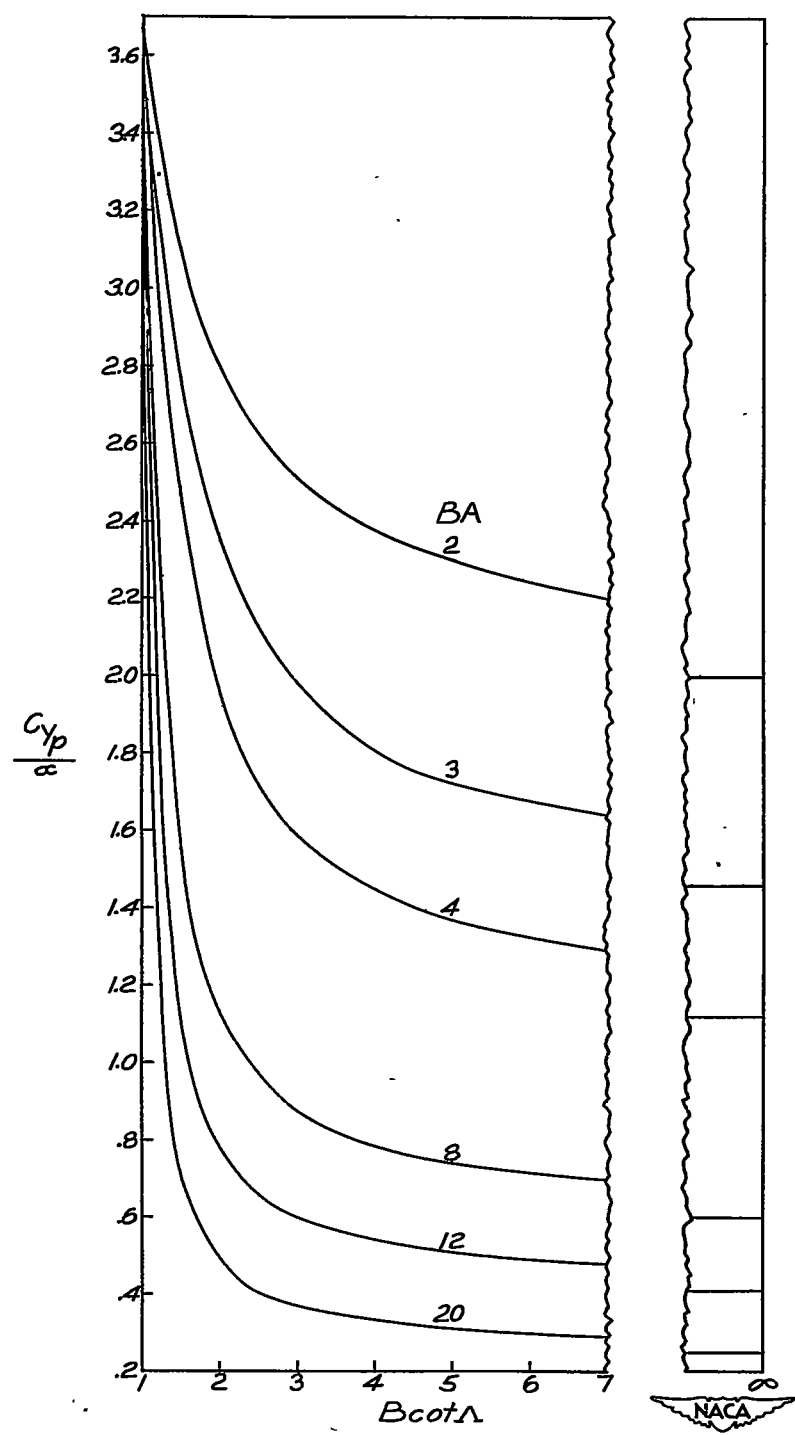
(d) Taper ratio $\lambda = 1.0$.

Figure 4.- Concluded.
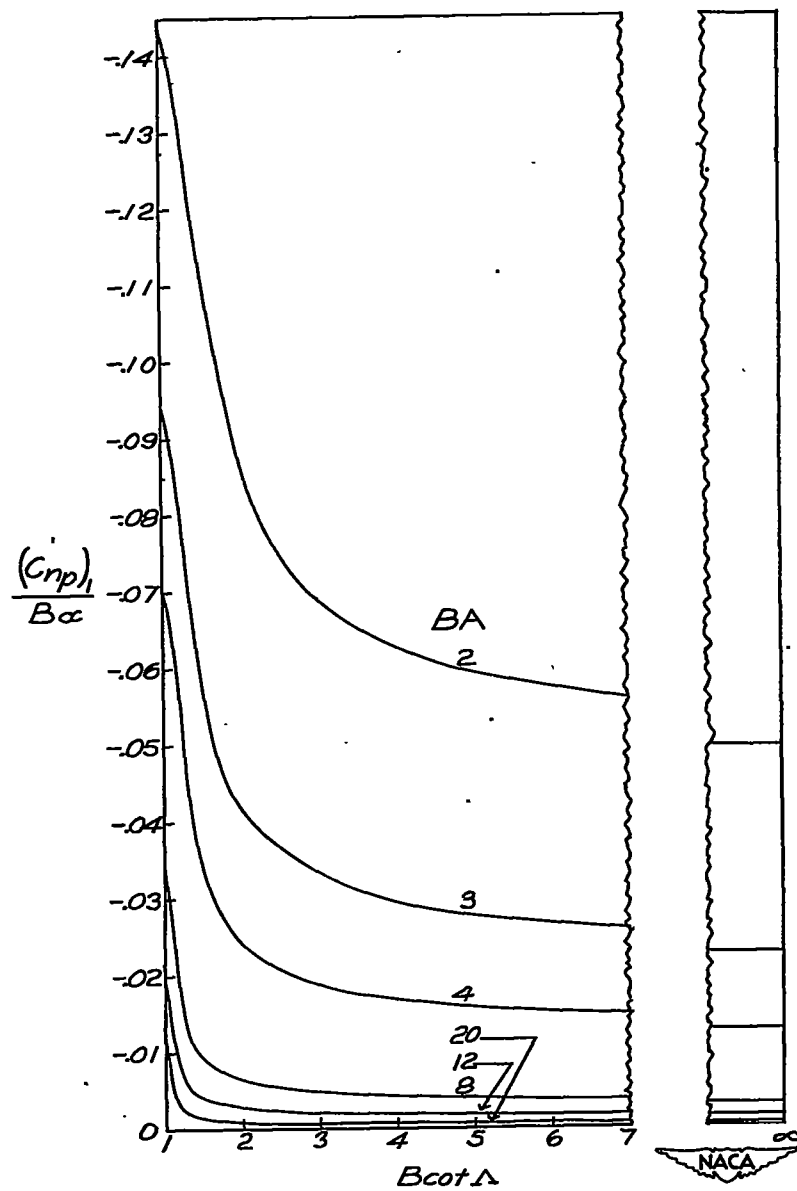
(a) Taper ratio $\lambda = 0.25$.

Figure 5.- Variation of $\left(C_{n_p}\right)_1 / B\alpha$ with sweepback-angle parameter for various aspect-ratio parameters and taper ratios. Derivative is with respect to body axes with origin at projection of leading edge of tip on center section (fig. 2(a)). (See equation (8) for conversion to stability axes.)
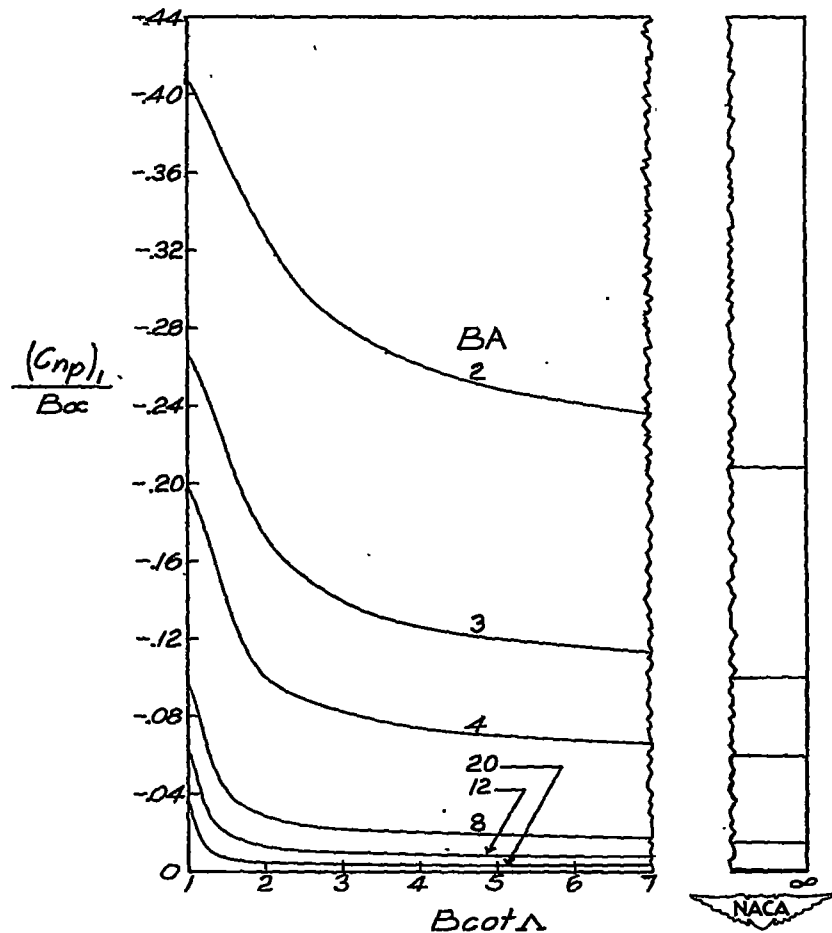
(b) Taper ratio $\lambda = 0.50.$

Figure 5.- Continued.
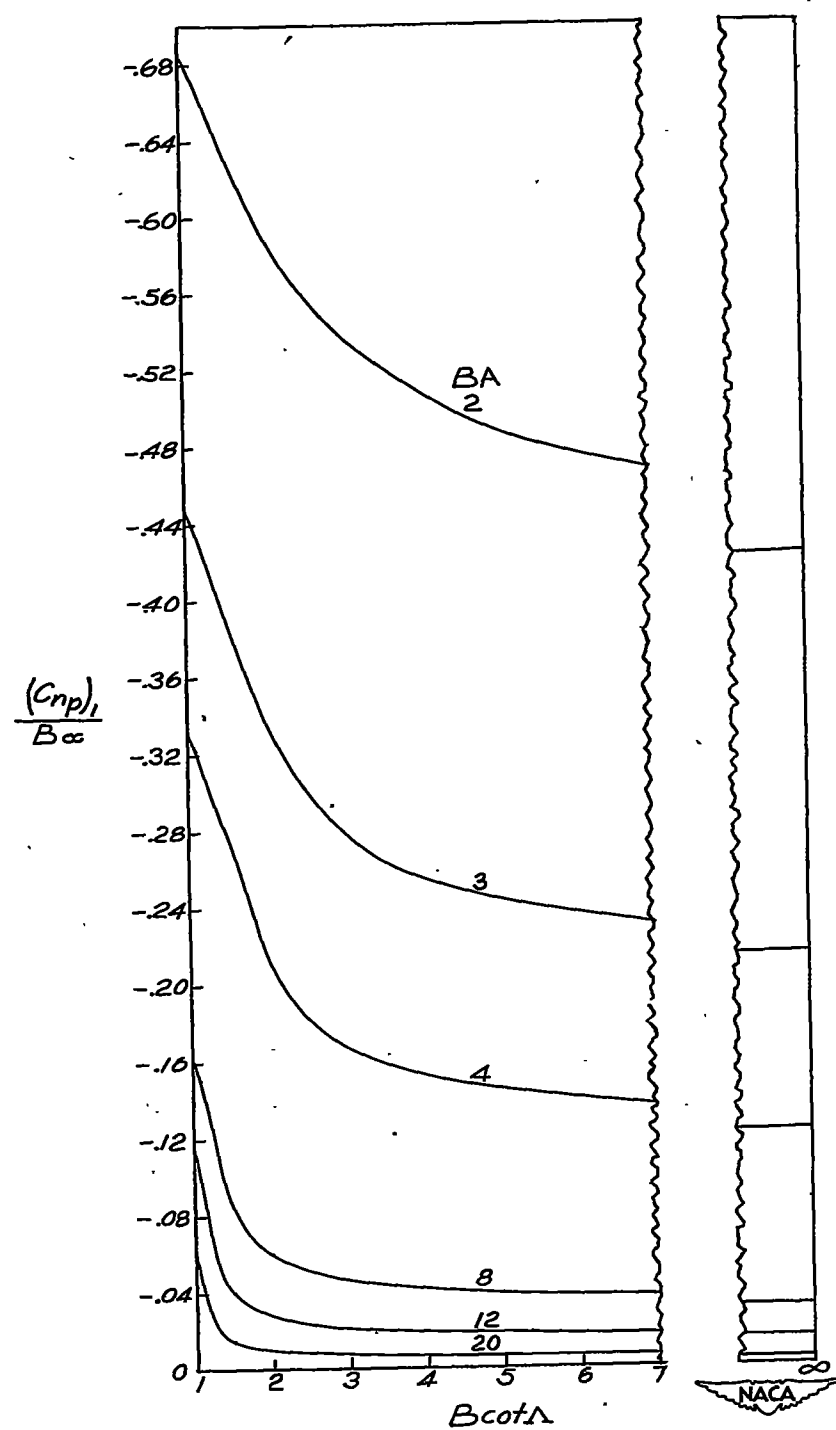
(c) Taper ratio $\lambda = 0.75$.

Figure 5.- Continued.
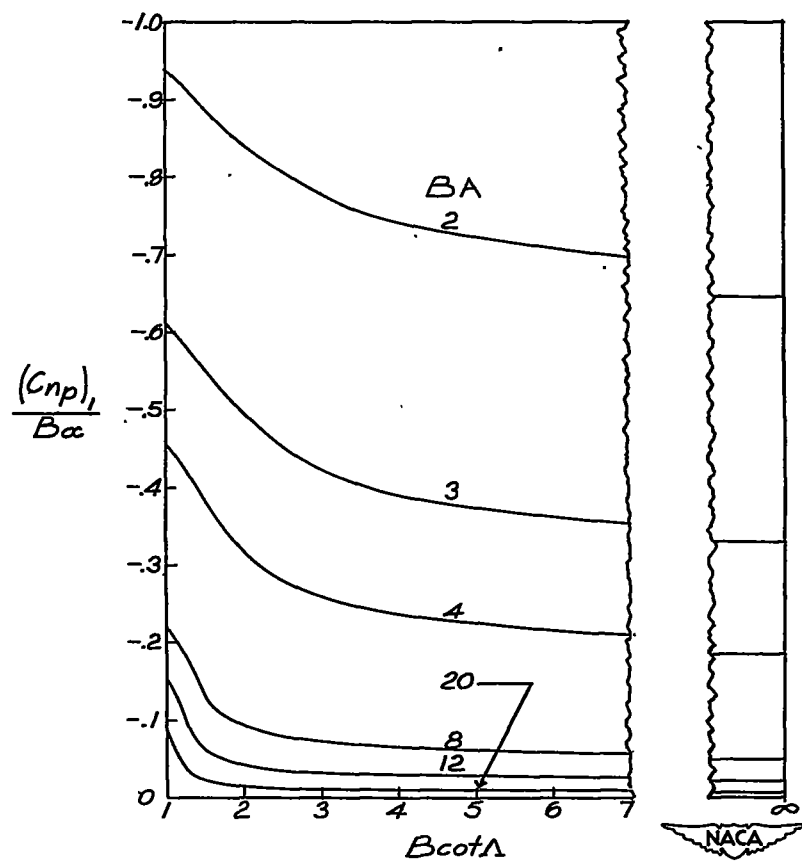
(d) Taper ratio　$\lambda = 1.0$.

Figure 5.- Concluded.
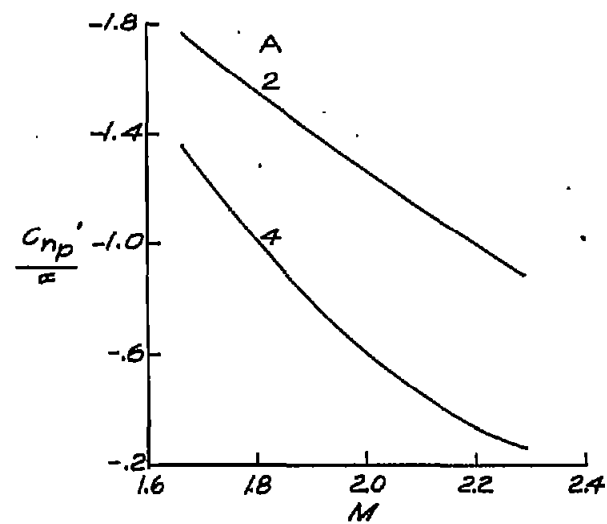
(a) Variation with Mach number.
$\Lambda = 53°$; $\lambda = 0.5$.
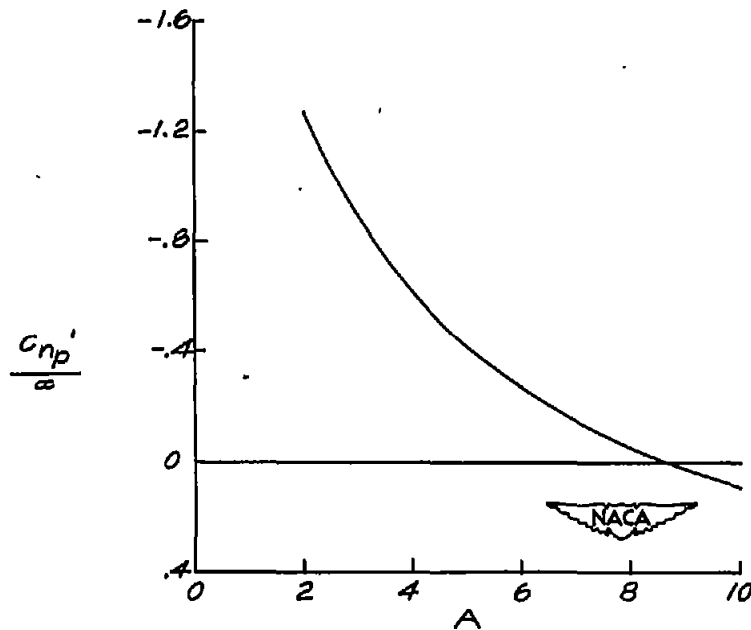
(b) Variation with aspect ratio.
$M = 2$; $\Lambda = 53°$; $\lambda = 0.5$.

Figure 6.- Illustrative variation of C_{n_p}'/α with Mach number, aspect ratio, sweep angle, and taper ratio. Derivative is with respect to stability axes with origin at leading edge of center section.
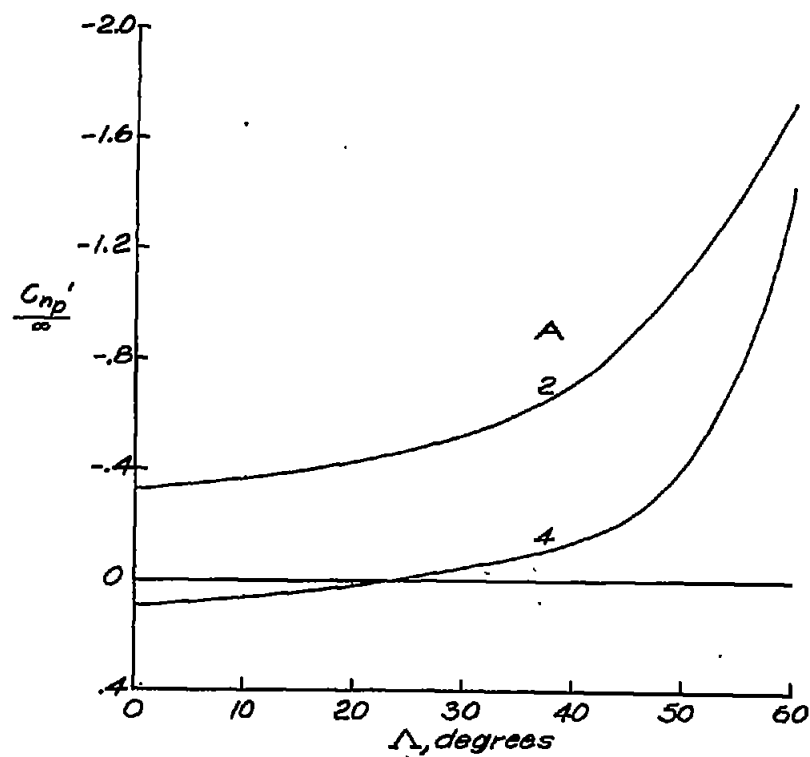
(c) Variation with angle of sweep.
M = 2; λ = 0.5.
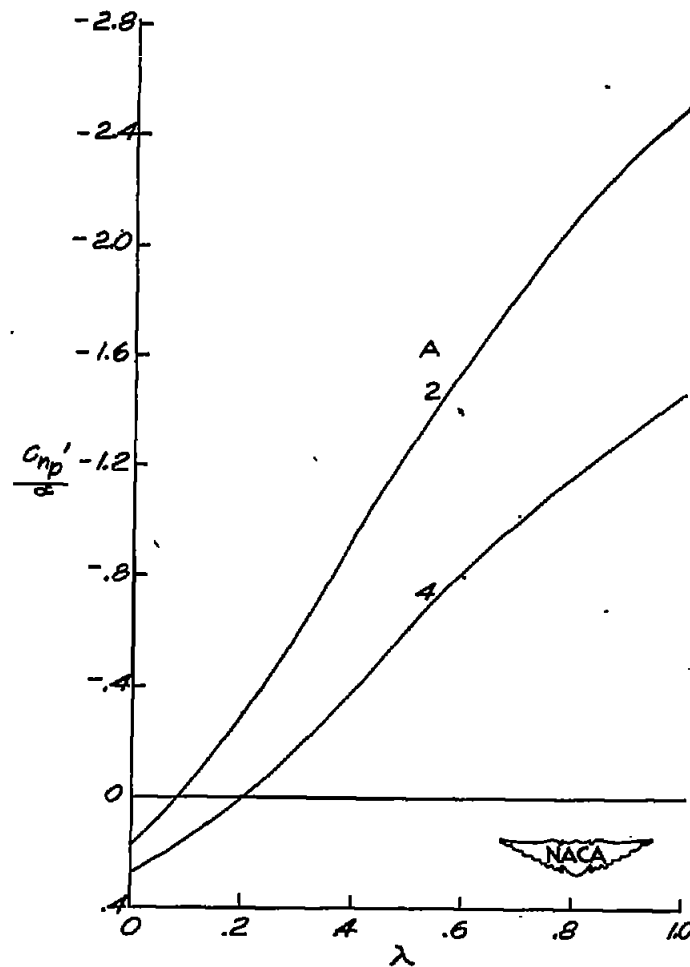
(d) Variation with taper ratio.
M = 2; Λ = 53°.

Figure 6.- Concluded.